OPINION PAPER

Which Earthquakes Are Expected to Exceed the Design Spectra?

Iunio Iervolino,[a] Massimiliano Giorgio,[b] and Pasquale Cito[a]

Extended recording coverage of contemporary seismic events allows a comparison of observed seismic actions with their counterparts used for design. Said comparison shows actions systematically exceeding design spectra. This paper discusses: (1) that considered exceedances can be anticipated by the probabilistic seismic hazard on the basis of which design actions are determined, (2) exceedances of elastic design actions are expected for earthquakes occurring close to the site even if their magnitude is far from the maximum magnitude considered in the hazard assessment, and (3) design spectra are likely to be exceeded in epicentral areas of earthquakes that occur frequently in the region where the code is enforced, but rarely occur close to the site under consideration. In fact, code-mandated protection against these earthquakes is factually warranted by the rarity with which they are expected to occur near the structure and other safety margins implicit to earthquake-resistant design. All these issues, addressed with reference to Italy, are discussed with the intent not to criticize the way spectra are determined, but rather to raise awareness and give a probabilistic measure about what to factually expect from state-of-the-art design at a national level. [DOI: 10.1193/032318EQS066O]

INTRODUCTION

The latest version of the Italian earthquake catalogue (CPTI15; Rovida et al. 2016), assigns moment magnitudes (Mw) in excess of 6 to 13 earthquakes in the 1915–2014 period, which translates to an average of 1 event every 8 years in the past century (this rough estimate does not take into consideration the occurrence of aftershocks or any issues of catalogue completeness). During the last decade, among the main (i.e., severely damaging) seismic sequences for the country, one counts L'Aquila (2009), Emilia (2012), and central Italy 2016–2017 (the latter not included in CPTI15), whose largest-magnitude earthquakes were Mw 6.3, Mw 6.1, and Mw 6.5, respectively.

In the same period as these events, an advanced seismic design code (Norme Tecniche per le Costruzioni (NTC); CS.LL.PP. 2008), largely based on Eurocode 8 (EC8; European Committee for Standardization (CEN) 2004), came into effect. According to NTC, seismic

[a] Dipartimento di Strutture per l'Ingegneria e l'Architettura, Università degli Studi di Napoli Federico II, via Claudio 21, 80125, Naples, Italy; Email: iunio.iervolino@unina.it (I. I.)
[b] Dipartimento di Ingegneria, Università degli Studi della Campania Luigi Vanvitelli, via Roma 29, 81031, Aversa, Italy

design actions for a specific location are determined on a probabilistic basis by means of uniform hazard spectra (UHS). In fact, the code prescribes the use of pseudoacceleration values that correspond to a given probability of being exceeded during a time interval that is assigned depending on the design life of the structure and its intended use. For example, in the case of an ordinary structure under design for the life-safety limit state, the elastic seismic action is typically represented by a spectrum whose ordinates (taken individually) are exceeded, on average, once every 475 years. The elastic spectra used for design have been calculated for the whole territory via the probabilistic seismic hazard analysis (PSHA) described in Stucchi et al. (2011). This may also be relevant on an international level because, according to Bommer and Acevedo (2004), "in nearly all current seismic design codes the earthquake actions are represented by an approximation to a uniform hazard spectrum obtained from a PSHA." Moreover, in general, the discussion herein applies to any design spectral acceleration derived directly from PSHA.

The recent seismic events that were mentioned at the beginning were of importance for earthquake engineering and engineering seismology because they provided an unprecedented level of instrumental recordings for the country (see, for example, Luzi et al. 2017). These data allow for a comparison of actually observed seismic actions with their code-prescribed counterparts that are used to design new structures. Said comparison has repeatedly shown, in the epicentral areas, registered seismic actions systematically exceeding design spectra. This, in turn, triggered a discussion on whether design actions behave as expected in real earthquakes (e.g., Panza et al. 2014, Zanini and Hofer 2017). In Iervolino (2013), the do's and don'ts of comparing seismic actions, which were recorded in one single earthquake, with their PSHA-evaluated counterparts were discussed. The objective of the present paper is to take this discussion further by considering multiple events in a large region (e.g., Italy). Given the nature of UHS, it is quantified in which earthquake scenario exceedance is more likely than nonexceedance. In fact, observed exceedances cannot be considered sufficient to claim that the code-mandated seismic actions underestimate the seismic hazard, and not only that, but rather, on the contrary, it should be made clear that such exceedances are a foreseeable consequence of the philosophy that underlies the definition of seismic actions in the code when it is based on probabilistic seismic hazard (e.g., Iervolino and Giorgio 2017). Note that issues classical PSHA does not account for, such as near-source directivity (e.g., Chioccarelli and Iervolino 2013), are not necessary to determine the conclusions of this study.

To prove this proposition, the starting point is the discussion of the seismic actions observed at the Amatrice recording site, which was in the epicentral area of the mainshock of the recent central Italy seismic sequence (e.g., Luzi et al. 2017) and is in one of the most hazardous regions in Italy. Subsequently, the fundamental principles behind the determination of UHS are briefly recounted. Still considering the Amatrice site as an example, the contribution to the probabilistic hazard of each magnitude-distance scenario is then discussed, showing that only earthquakes occurring close to the site tend to be relevant. Among these close-by earthquakes, the more frequent events, when they occur, are unlikely to cause exceedance of the design acceleration. Conversely, those that rarely occur close to the site (e.g., within 20 km), even if their magnitude is relatively far from the maximum considered magnitude (i.e., events that can occur relatively frequently over a large region), can have a high probability of provoking such an exceedance. Consequently,

for constructions subjected to one of these events, safety is basically warranted by the rarity with which it is expected that the epicenter occurs close to the structure; this can be a relevant issue from the structural engineering perspective. In fact, exceedance of elastic design actions does not necessarily imply structural failure, as seismic design is expected to provide further safety margins (although such margins are generally not explicitly controlled; e.g., Iervolino et al. 2017). Finally, the discussion is taken at the national level, mapping the minimum magnitudes that, in the case of occurrence close to the site of interest, have at least 50% probability of exceeding selected spectral ordinates of site-specific UHS. To comment the map, the low-hazard site of Milan is compared to Amatrice. Final remarks close the study.

PROBABILISTIC HAZARD–BASED SPECTRA

Generally, in seismic codes, the earthquake's intensity for verification of a structure against a given seismic performance objective (i.e., the limit state) is represented by the ordinates of a pseudoacceleration response spectrum applicable at the construction site and referring to a given damping factor. Herein, following a common notation, these ordinates will be indicated as $Sa(T)$, where T is the arbitrary natural vibration period of a linear-elastic oscillator.

Figure 1a shows the spectra of the horizontal components of the seismic ground motion recorded at the site of Amatrice (AMT station of the Rete Accelerometrica Nazionale; Dolce 2011) during the largest-magnitude earthquake (Mw 6.5; 30 October 2016) of the central Italy sequence. The site was about 10 km from the source, in terms of Joyner

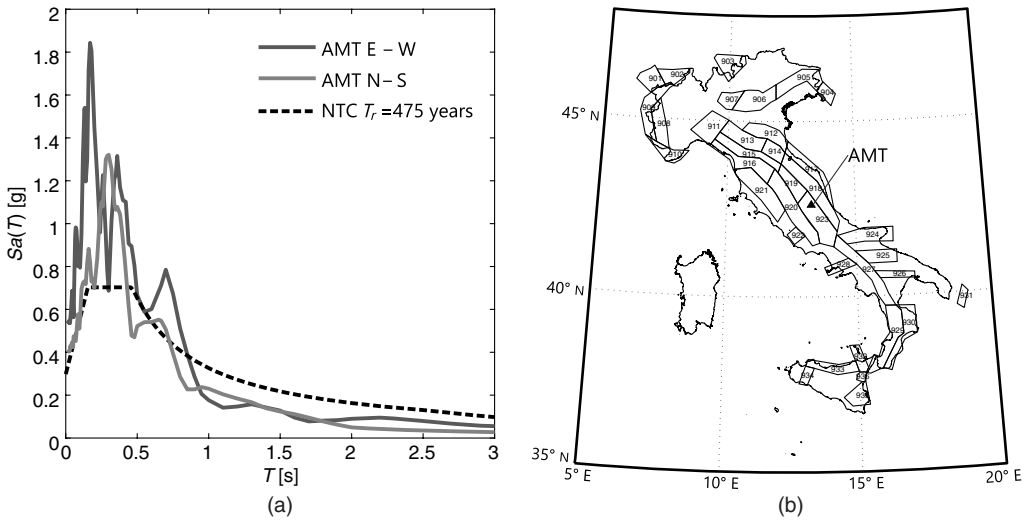

Figure 1. (a) East-west (E-W) and north-south (N-S) spectra recorded at Amatrice (AMT station) during the 30 October 2016 Mw 6.5 earthquake, and code spectra for $T_r = 475$ years (site class is B according EC8 classification, as reported for AMT at ITACA; Luzi et al. 2008). (b) The seismic source zones to determine design actions, according to NTC.

and Boore distance (Joyner and Boore 1981). The figure also shows the spectrum for the life-safety design of an ordinary structure according to NTC. The code spectrum refers to the same EC8 soil site class of the recording station. Such a spectrum is computed in such a way that any ordinate (individually) is exceeded, on average, once every certain number of years, said number being referred to as the return period (T_r), with the spectrum in the figure corresponding to $T_r = 475$ years. This T_r is taken as a reference herein, although the conclusions are qualitatively independent of it. (To be precise, in NTC, spectra for A-type site class are UHS approximated via the EC8-type functional form. Spectra for other site classes are obtained by applying correction factors to the A-type UHS. Also note that code UHS are developed considering the maximum acceleration between the two horizontal components as the ground motion intensity measure.)

One notices that the design actions have been greatly exceeded over a relatively ample interval of natural vibration periods of structural interest, and this is not an exceptional case either in the 2016 central Italy seismic sequence nor in other significant seismic events, such as L'Aquila 2009 (Masi et al. 2011) and Emilia 2012 (Chioccarelli et al. 2012).

As mentioned, the elastic design spectra of the NTC are, actually, approximations of UHS from PSHA (e.g., McGuire 2004), which consists of the calculation of the annual rate, $\lambda_{Sa(T)>sa}$, of earthquakes causing exceedance of a threshold intensity value, say, sa. The basic equation of PSHA is the hazard integral, as per Equation 1:

$$\lambda_{Sa(T)>sa} = \sum_{i=1}^{s} \nu_i \cdot \int_{r_{\min}}^{r_{\max}} \int_{m_{\min}}^{m_{\max}} P[Sa(T) > sa \,|\, M = m, R = r] \cdot f_{M,R,i}(m,r) \cdot dm \cdot dr \quad (1)$$

In the equation, it is considered that the site is affected by a number (s) of seismic sources; e.g., the seismic source zones. Each source is characterized by the annual rate, ν_i, $i = \{1, 2, \ldots, s\}$, of earthquakes between the minimum magnitude of interest $(m_{\min})$ and the maximum magnitude considered possible for the zone $(m_{\max})$. The term $P[Sa(T) > sa \,|\, M = m, R = r]$, generally provided by ground motion prediction equations (GMPEs), is the conditional probability that an earthquake, with magnitude $M = m$ and source-to-site distance $R = r$, causes exceedance of sa. GMPEs usually include other covariates, which usually are not random variables (RVs), such as the soil site class. The GMPE is kept the same for different zones when the seismotectonic structure is homogeneous. Finally, $f_{M,R,i}(m,r)$ is the joint probability density function (PDF) of the earthquake magnitude and distance RVs for the ith zone. Usually these RVs are assumed, for each source, to be stochastically independent, thus $f_{M,R,i}(m,r) = f_{M,i}(m) \cdot f_{R,i}(r)$. A typical working hypothesis in PSHA (also used herein) is that the distance PDF, $f_{R,i}(r)$, derives from the uniform distribution of earthquake location, while the magnitude PDF, $f_{M,i}(m)$, tends to be such that the largest is m, the smaller is the probability of observing earthquakes with $M > m$ (Gutenberg and Richter 1944). Computing the hazard integral for a series of sa values and plotting $\lambda_{Sa(T)>sa}$ against them, provides the so-called hazard curve.

Returning to the Amatrice case, Figure 2a shows a series of hazard curves corresponding to a set of spectral ordinates, $Sa(T), T \in (0\,\text{s}, 2\,\text{s})$, for the site. The curves were derived via

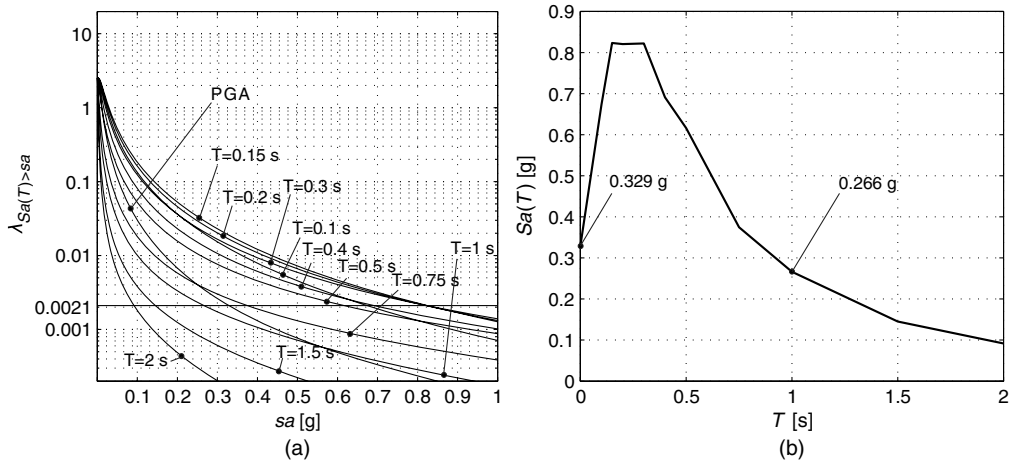

Figure 2. (a) Hazard curves for B soil site class at Amatrice; (b) UHS corresponding to 475 years.

the REASSESS software (Chioccarelli et al. 2019) considering the input data of the branch named "921" of the logic tree that was used to build the Italian hazard map that the seismic code is based on. This branch features 36 seismic source zones (numbered from 901 to 936, not to be confused with the name of the logic tree branch) of the model in Meletti et al. (2008), shown in Figure 1b, and the GMPE of Ambraseys et al. (1996); see Stucchi et al. (2011) for details. The rates of earthquake occurrence are given per surface-waves magnitude bins in Table 1 (Carlo Meletti, *pers. comm.*; these rates account for the fact that it is assumed that only the sources within 230 km from the site of Amatrice are assumed to contribute to its hazard).

It is well known that, by virtue of the relation between annual exceedance rate and return period in the classical hypotheses of PSHA (e.g., Cornell 1968), to calculate the UHS whose ordinates are exceeded, on average, once every 475 years, it is sufficient to enter the vertical axis of every hazard curve with $\lambda_{Sa(T)>sa} = 1/475 = 0.0021$, and plot them versus the natural vibration period. This spectrum is shown for the site of Amatrice in Figure 2b; in the following, its ordinates will be generically referred to as $sa_{T_r=475}$.

Note that the spectrum given in Figure 2b differs from that of Figure 1a because the former was computed with only a single branch of the logic tree. Moreover, as discussed, design spectra for soil classes different from A-type (rock) are obtained from rock UHS via amplification coefficients. None of these issues affect the discussion in the paper.

CONTRIBUTION OF M-R SCENARIOS TO HAZARD

It is now useful to recall some very basic concepts related to PSHA, by rewriting the hazard integral as in Equation 2, where $\nu_{M=m,R=r} \cdot dr \cdot dm = \sum_{i=1}^{s} \nu_i \cdot f_{M,R,i}(m,r) \cdot dr \cdot dm$

Table 1. Magnitude annual rates for the seismic source zones of Meletti et al. (2008) as per branch 921 of the logic tree of Stucchi et al. (2011)

	Magnitude bin										
Zone	4.15–4.45	4.45–4.75	4.75–5.05	5.05–5.35	5.35–5.65	5.65–5.95	5.95–6.25	6.25–6.55	6.55–6.85	6.85–7.15	7.15–7.45
912	4.8E−02	1.2E−02	1.1E−02	1.5E−02	2.1E−03	2.8E−03	1.2E−03	0.0E+00	0.0E+00	0.0E+00	0.0E+00
914	8.4E−02	6.6E−02	1.5E−02	8.5E−03	2.1E−03	5.7E−03	1.4E−03	0.0E+00	0.0E+00	0.0E+00	0.0E+00
915	1.8E−01	7.6E−02	4.0E−02	0.0E+00	4.2E−03	4.2E−03	1.4E−03	1.4E−03	0.0E+00	0.0E+00	0.0E+00
916	4.6E−02	3.1E−02	8.5E−03	4.2E−03	2.1E−03	0.0E+00	0.0E+00	0.0E+00	0.0E+00	0.0E+00	0.0E+00
917	5.4E−02	3.0E−02	1.1E−02	8.5E−03	1.1E−02	6.4E−03	1.2E−03	0.0E+00	0.0E+00	0.0E+00	0.0E+00
918	1.5E−01	2.3E−02	1.7E−02	5.7E−03	8.5E−03	6.4E−03	4.2E−03	1.4E−03	0.0E+00	0.0E+00	0.0E+00
919	1.3E−01	5.3E−02	3.0E−02	1.1E−02	4.2E−03	7.1E−03	4.3E−03	2.5E−03	0.0E+00	0.0E+00	0.0E+00
920	1.8E−01	6.9E−02	5.7E−02	8.5E−03	0.0E+00	0.0E+00	0.0E+00	0.0E+00	0.0E+00	0.0E+00	0.0E+00
921	1.8E−01	8.4E−02	2.5E−02	8.5E−03	2.1E−03	2.8E−03	0.0E+00	0.0E+00	0.0E+00	0.0E+00	0.0E+00
922	4.6E−02	2.3E−02	1.7E−02	4.2E−03	0.0E+00	0.0E+00	0.0E+00	0.0E+00	0.0E+00	0.0E+00	0.0E+00
923	4.1E−01	9.9E−02	7.7E−02	2.3E−02	8.5E−03	1.1E−02	2.1E−03	5.7E−03	4.3E−03	1.4E−03	1.4E−03
924	6.9E−02	3.8E−02	3.7E−02	2.8E−02	1.4E−02	0.0E+00	4.2E−03	0.0E+00	1.7E−03	0.0E+00	0.0E+00
925	4.6E−02	1.5E−02	4.7E−03	0.0E+00	0.0E+00	0.0E+00	0.0E+00	3.3E−03	1.7E−03	0.0E+00	0.0E+00
927	2.2E−01	5.6E−02	5.1E−02	9.3E−03	4.7E−03	6.4E−03	2.1E−03	4.2E−03	6.6E−03	6.6E−03	0.0E+00
928	1.5E−02	1.5E−02	1.9E−02	0.0E+00	4.2E−03	2.1E−03	0.0E+00	0.0E+00	0.0E+00	0.0E+00	0.0E+00

represents the rate of earthquakes of magnitude within $(m,m+dm)$ at a distance within $(r,r+dr)$, considering all seismic sources:

$$\lambda_{Sa(T)>sa} = \int_{r_{\min}}^{r_{\max}} \int_{m_{\min}}^{m_{\max}} P[Sa(T) > sa \,|\, M = m,R = r] \cdot \nu_{M=m,R=r} \cdot dm \cdot dr \tag{2}$$

In fact, the hazard integral can be further compacted as in Equation 3, where $\lambda_{Sa(T)>sa,M=m,R=r} \cdot dm \cdot dr = P[Sa(T) > sa \,|\, M = m,R = r] \cdot \nu_{M=m,R=r} \cdot dm \cdot dr$ is the rate of earthquakes of magnitude within $(m,m+dm)$ at a distance within $(r,r+dr)$, causing exceedance of the intensity threshold. In other words, $\lambda_{Sa(T)>sa,M=m,R=r} \cdot dm \cdot dr$ is the contribution to the hazard of the $\{m,r\}$ scenario.

$$\lambda_{Sa(T)>sa} = \int_{r_{\min}}^{r_{\max}} \int_{m_{\min}}^{m_{\max}} \lambda_{Sa(T)>sa,M=m,R=r} \cdot dm \cdot dr \tag{3}$$

For each ordinate of the $T_r = 475$ years UHS, it holds by definition that $\lambda_{Sa(T)>sa} = 0.0021$, and then none of the aforementioned single contributions can exceed this value; i.e., Equation 4. In the equation, and in the following, Δm and Δr, which are small yet finite $\{m,r\}$ bins, replace dm and dr, respectively.

$$\begin{aligned} \lambda_{Sa(T)>sa,M=m,R=r} \cdot \Delta m \cdot \Delta r &= P[Sa(T) > sa \,|\, M = m,R = r] \cdot \nu_{M=m,R=r} \cdot \Delta m \cdot \Delta r \\ &\leq 0.0021, \quad \forall\{m,r\} \end{aligned} \tag{4}$$

Given the source-to-site-distance, because lower magnitude earthquakes are, typically, more frequent than higher magnitudes (see, for example, Table 1), the constraint in Equation 4 is satisfied in a way that when low-magnitude events occur, they have a low probability of exceeding the acceleration threshold. Conversely, higher-magnitude earthquakes, being rarer (i.e., with low recurrence rate), can have high exceedance probability; i.e., $P[Sa(T) > sa \,|\, M = m,R = r]$ can even approach one.

To better illustrate the point, Figure 3 provides a representation of the hazard integral via the individual contributions of magnitude and distance scenarios. In particular, the $Sa(T = 1\,\text{s})$ spectral ordinate from Figure 2b is considered; i.e., $sa_{T_r=475} = 0.266\,\text{g}$. The choice of this spectral ordinate and return period is arbitrary and suggested by the fact that 1 s is in a range of the spectrum of engineering interest, and 475 years is the return period for the life-safety limit state design of ordinary constructions in the Italian code; however, the same discussion applies to any other spectral ordinate or return period, as discussed in the following. Figure 3c provides the annual rates $\lambda_{Sa(T=1\,\text{s})>sa_{T_r=475},M=m,R=r} \cdot \Delta m \cdot \Delta r$, that is, the average number of earthquakes per year causing exceedance of 0.266 g for each magnitude-distance bin. By definition, the sum of these rates over all the bins is equal to $\lambda_{Sa(T=1\,\text{s})>sa_{T_r=475}} = 0.0021$. Note that the table factually represents the distribution of magnitude and distance one obtains from hazard disaggregation (e.g., Iervolino et al. 2011) multiplied by 0.0021. Figure 3a gives the annual occurrence rates of earthquakes corresponding to each bin; i.e., $\nu_{M=m,R=r} \cdot \Delta m \cdot \Delta r$. Finally, Figure 3b provides the conditional

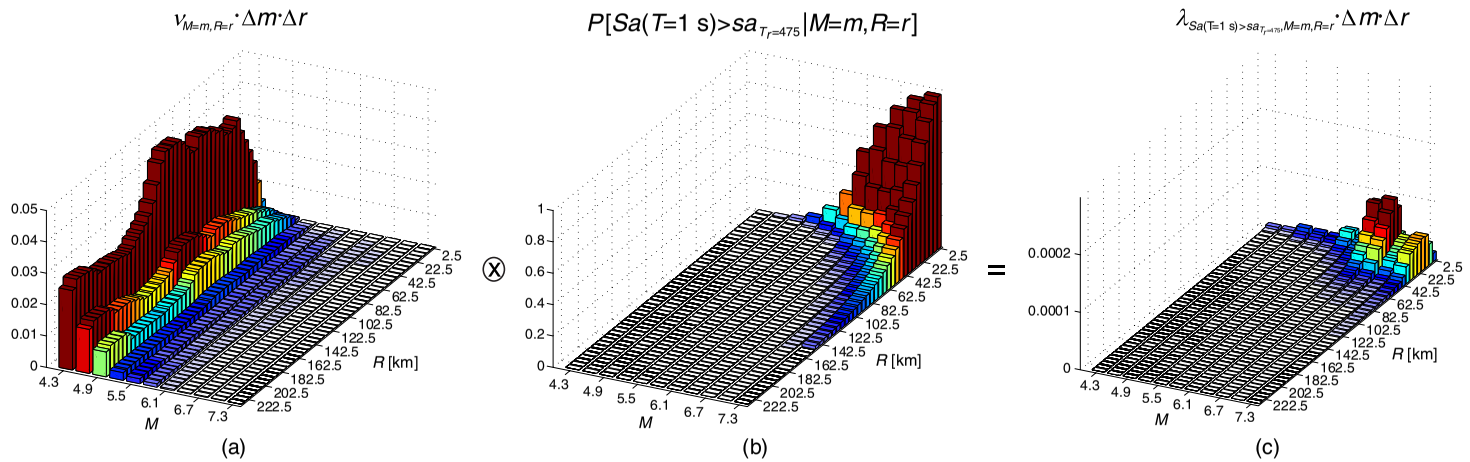

Figure 3. Magnitude and distance dissection of the hazard for Amatrice in terms of $T = 1$ s spectral acceleration with an exceedance return period equal to 475 years, that is, 0.266 g. (a) Rates of occurrence (1/year); (b) probability of exceedance; (c) product of the previous two (1/year). Integrating (c) yields 0.0021=1/475. Distance in the graphs is epicentral.

probability that earthquakes corresponding to each $\{m,r\}$ scenario cause exceedance of 0.266 g, that is, $P[Sa(T = 1\,\mathrm{s}) > sa_{T_r=475} \,|\, M = m,R = r]$. Bin by bin, the values in Figure 3c coincide with those of Figure 3a multiplied by those in Figure 3b.

For Amatrice, the $\nu_{M=m,R=r} \cdot \Delta m \cdot \Delta r$ rates in Figure 3a rapidly decrease with increasing magnitude, regardless of the distance. Looking at the dependence on R, it appears that the rates tend to decrease with the distance approaching zero. Consequently, there are many scenarios with small-to-very-small occurrence rates (i.e., white bins in the figure). These correspond to high magnitudes at any distance, or relatively rare magnitudes at small distances. Figure 3b provides the effect of the $\{m,r\}$ scenarios in terms of probability of exceeding the UHS ordinate of interest. Because such a probability increases with increasing magnitude and decreasing distance, as expected from GMPEs, there are several bins with large exceedance probability conditional to the occurrence of the M and R scenario. Indeed, the conditional exceedance probability starts to be significant at $M \geq 5, R \leq 5$ km, but is large up to $R \approx 50$ km, depending on the magnitude. Finally, recalling that Figure 3c reports the contribution of the magnitude-distance scenarios to hazard, weighing the exceedance probability of each scenario by its occurrence rate, it appears that the $\{m,r\}$ bins that give the largest contributions for Amatrice are close earthquakes because of their large $P[Sa(T = 1\,\mathrm{s}) > sa_{T_r=475} \,|\, M = m,R = r]$ or relatively significant $\nu_{M=m,R=r} \cdot \Delta m \cdot \Delta r$, or both.

CLOSE-BY EARTHQUAKES

In this section, the earthquakes that contribute most to the hazard are analyzed. They are, almost exclusively, the earthquakes within 50 km of the site.

This can be quantitatively evaluated via Table 2, which is the tabular representation of Figure 3c. Summing up the rate values from cells up to $R \leq 50$ km gives 0.00194, which means that the earthquakes occurring within this distance represent more than 90% of the $Sa(T = 1\,\mathrm{s})$ hazard with an exceedance return period $T_r = 475$ years in Amatrice, which is a common situation for sites within a source zone that dominates the hazard disaggregation; e.g., Iervolino et al. (2011).

Further insights can be now obtained by dissecting the contributions of these close-by scenarios. It can be seen from Figure 3c that there are different magnitudes with similar contributions. For example, an earthquake of magnitude $\Delta m \equiv 5.65 \leq M < 5.95$ (i.e., $M \approx 5.8$) at a distance $\Delta r \equiv 5\,\mathrm{km} \leq R < 10\,\mathrm{km}$ (i.e., $R \approx 7\,\mathrm{km}$) has $\lambda_{Sa(T)>sa_{T_r=475},M=m,R=r} \cdot \Delta m \cdot \Delta r \approx 3\mathrm{E}-5$ (1/year), which is about the same of an earthquake $\Delta m \equiv 6.85 \leq M < 7.15$ (i.e., $M \approx 7$) at distance $R \approx 7$ km. However, this equivalent contribution to the hazard arises from very different occurrence rates and conditional exceedance probabilities, as can be seen in Table 3, where the values from the three panels in Figure 3 are given for the two scenarios. Despite the same threshold exceedance rate, the two scenarios are very different in rarity, as expected. The one with the lower magnitude, $M \approx 5.8$, is about 10 times more frequent than the larger; i.e., $M \approx 7$. When an earthquake $M \approx 5.8$ at $R \approx 7$ km occurs, it only has a 10% probability of exceeding the $Sa(T = 1\,\mathrm{s})$ ordinate of the $T_r = 475$ years UHS for Amatrice; i.e., in case of occurrence, there is a 90% chance that the UHS will not be exceeded at that ordinate. Conversely, when an $M \approx 7$ earthquake occurs at $R \approx 7$ km from Amatrice, then the probability of exceeding $sa_{T_r=475}$ is about 90%.

Table 2. Decomposition of the $T_r = 475$ years $Sa(T = 1\,\mathrm{s})$ hazard calculation in magnitude and source-to-site distance bins showing the contribution (annual rates) of each scenario; i.e., $\lambda_{Sa(T=1\,\mathrm{s})>sa_{T_r=475},M=m,R=r} \cdot \Delta m \cdot \Delta r$

	Δm										
Δr	4.15–4.45	4.45–4.75	4.75–5.05	5.05–5.35	5.35–5.65	5.65–5.95	5.95–6.25	6.25–6.55	6.55–6.85	6.85–7.15	7.15–7.45
0–5	5.2E−06	5.2E−06	1.4E−05	1.2E−05	1.1E−05	2.6E−05	1.2E−05	4.2E−05	3.8E−05	1.4E−05	1.4E−05
5–10	1.8E−06	2.3E−06	8.0E−06	8.4E−06	9.5E−06	2.9E−05	2.3E−05	9.2E−05	8.8E−05	3.4E−05	3.6E−05
10–15	3.7E−07	6.2E−07	2.7E−06	3.6E−06	5.0E−06	1.9E−05	2.0E−05	9.6E−05	1.1E−04	4.6E−05	5.4E−05
15–20	9.1E−08	1.8E−07	9.3E−07	1.5E−06	2.7E−06	1.1E−05	1.6E−05	7.1E−05	8.9E−05	4.3E−05	5.6E−05
20–25	2.4E−08	6.1E−08	3.6E−07	6.4E−07	1.6E−06	6.7E−06	1.3E−05	5.1E−05	6.8E−05	3.7E−05	5.2E−05
25–30	5.5E−09	2.4E−08	1.6E−07	3.2E−07	9.3E−07	4.2E−06	9.9E−06	3.7E−05	5.3E−05	3.1E−05	4.9E−05
30–35	6.3E−10	9.7E−09	7.9E−08	1.8E−07	5.8E−07	2.8E−06	7.4E−06	2.9E−05	4.4E−05	2.8E−05	4.6E−05
35–40	3.0E−11	3.4E−09	3.8E−08	9.1E−08	3.4E−07	1.7E−06	6.0E−06	1.8E−05	2.5E−05	1.7E−05	2.9E−05
40–45	0.0E+00	1.1E−09	2.0E−08	5.1E−08	2.1E−07	1.2E−06	5.2E−06	1.2E−05	1.2E−05	8.6E−06	1.6E−05
45–50	0.0E+00	2.5E−10	1.0E−08	3.0E−08	1.4E−07	7.9E−07	4.0E−06	8.6E−06	7.1E−06	5.4E−06	1.1E−05
50–55	0.0E+00	5.0E−11	5.6E−09	1.9E−08	9.6E−08	5.5E−07	2.9E−06	6.4E−06	5.5E−06	4.5E−06	9.3E−06
55–60	0.0E+00	4.9E−11	3.2E−09	1.6E−08	9.7E−08	4.8E−07	2.1E−06	4.4E−06	4.1E−06	3.5E−06	7.5E−06
60–65	0.0E+00	1.3E−11	1.8E−09	1.2E−08	8.2E−08	3.9E−07	1.5E−06	3.2E−06	3.2E−06	2.9E−06	6.5E−06
65–70	0.0E+00	0.0E+00	8.5E−10	8.2E−09	6.2E−08	3.0E−07	1.2E−06	2.4E−06	2.6E−06	2.4E−06	5.6E−06
70–75	0.0E+00	0.0E+00	2.8E−10	4.6E−09	3.5E−08	1.8E−07	7.9E−07	1.8E−06	2.1E−06	2.0E−06	4.7E−06
75–80	0.0E+00	0.0E+00	1.2E−10	2.8E−09	2.4E−08	1.3E−07	5.8E−07	1.4E−06	1.6E−06	1.6E−06	4.1E−06
80–85	0.0E+00	0.0E+00	4.9E−11	1.8E−09	1.7E−08	9.5E−08	4.3E−07	1.1E−06	1.3E−06	1.4E−06	3.5E−06
85–90	0.0E+00	0.0E+00	2.0E−11	1.2E−09	1.3E−08	7.2E−08	3.3E−07	8.3E−07	1.1E−06	1.2E−06	3.0E−06
90–95	0.0E+00	0.0E+00	6.9E−12	7.7E−10	9.3E−09	5.5E−08	2.5E−07	6.6E−07	9.4E−07	1.0E−06	2.8E−06
95–100	0.0E+00	0.0E+00	0.0E+00	5.0E−10	7.2E−09	4.4E−08	2.0E−07	5.4E−07	8.2E−07	9.2E−07	2.6E−06
100–105	0.0E+00	0.0E+00	0.0E+00	3.0E−10	5.3E−09	3.4E−08	1.6E−07	4.5E−07	7.2E−07	8.3E−07	2.4E−06

105–110	0.0E+00	0.0E+00	0.0E+00	1.8E−10	4.1E−09	2.7E−08	1.2E−07	3.6E−07	6.3E−07	7.4E−07	2.2E−06
110–115	0.0E+00	0.0E+00	0.0E+00	1.0E−10	2.9E−09	2.0E−08	8.9E−08	2.9E−07	5.6E−07	6.6E−07	2.0E−06
115–120	0.0E+00	0.0E+00	0.0E+00	6.1E−11	2.1E−09	1.6E−08	6.9E−08	2.4E−07	4.8E−07	5.9E−07	1.8E−06
120–125	0.0E+00	0.0E+00	0.0E+00	3.3E−11	1.5E−09	1.2E−08	5.3E−08	1.9E−07	3.9E−07	5.2E−07	1.5E−06
125–130	0.0E+00	0.0E+00	0.0E+00	1.9E−11	1.1E−09	9.3E−09	4.4E−08	1.5E−07	3.4E−07	6.1E−07	1.2E−06
130–135	0.0E+00	0.0E+00	0.0E+00	9.1E−12	8.3E−10	6.9E−09	3.8E−08	1.2E−07	3.3E−07	6.8E−07	8.0E−07
135–140	0.0E+00	0.0E+00	0.0E+00	3.4E−12	6.5E−10	5.5E−09	3.3E−08	9.4E−08	3.0E−07	7.4E−07	5.0E−07
140–145	0.0E+00	0.0E+00	0.0E+00	6.8E−13	4.9E−10	4.3E−09	2.8E−08	7.4E−08	2.8E−07	7.5E−07	2.7E−07
145–150	0.0E+00	0.0E+00	0.0E+00	0.0E+00	3.6E−10	3.3E−09	2.4E−08	5.7E−08	2.6E−07	7.6E−07	1.0E−07
150–155	0.0E+00	0.0E+00	0.0E+00	0.0E+00	2.7E−10	2.6E−09	2.0E−08	4.3E−08	2.4E−07	7.2E−07	0.0E+00
155–160	0.0E+00	0.0E+00	0.0E+00	0.0E+00	1.9E−10	2.1E−09	1.6E−08	3.4E−08	2.2E−07	6.5E−07	0.0E+00
160–165	0.0E+00	0.0E+00	0.0E+00	0.0E+00	1.4E−10	1.7E−09	1.4E−08	2.7E−08	2.0E−07	5.7E−07	0.0E+00
165–170	0.0E+00	0.0E+00	0.0E+00	0.0E+00	1.0E−10	1.5E−09	1.2E−08	2.1E−08	1.8E−07	5.0E−07	0.0E+00
170–175	0.0E+00	0.0E+00	0.0E+00	0.0E+00	6.5E−11	1.3E−09	1.1E−08	1.7E−08	1.6E−07	4.4E−07	0.0E+00
175–180	0.0E+00	0.0E+00	0.0E+00	0.0E+00	4.7E−11	1.2E−09	9.4E−09	1.3E−08	1.4E−07	3.9E−07	0.0E+00
180–185	0.0E+00	0.0E+00	0.0E+00	0.0E+00	3.6E−11	1.0E−09	8.2E−09	1.1E−08	1.3E−07	3.5E−07	0.0E+00
185–190	0.0E+00	0.0E+00	0.0E+00	0.0E+00	1.9E−11	8.5E−10	7.0E−09	9.1E−09	1.1E−07	3.1E−07	0.0E+00
190–195	0.0E+00	0.0E+00	0.0E+00	0.0E+00	1.2E−11	6.7E−10	6.1E−09	7.9E−09	9.5E−08	2.8E−07	0.0E+00
195–200	0.0E+00	0.0E+00	0.0E+00	0.0E+00	5.6E−12	5.4E−10	5.4E−09	6.7E−09	8.3E−08	2.5E−07	0.0E+00
200–205	0.0E+00	0.0E+00	0.0E+00	0.0E+00	2.2E−12	4.6E−10	4.7E−09	6.3E−09	7.3E−08	2.2E−07	0.0E+00
205–210	0.0E+00	0.0E+00	0.0E+00	0.0E+00	1.3E−12	3.7E−10	4.2E−09	6.9E−09	7.1E−08	2.0E−07	0.0E+00
210–215	0.0E+00	0.0E+00	0.0E+00	0.0E+00	0.0E+00	2.8E−10	3.7E−09	7.2E−09	6.7E−08	1.8E−07	0.0E+00
215–220	0.0E+00	0.0E+00	0.0E+00	0.0E+00	0.0E+00	2.3E−10	3.3E−09	7.3E−09	6.2E−08	1.6E−07	0.0E+00
220–225	0.0E+00	0.0E+00	0.0E+00	0.0E+00	0.0E+00	1.8E−10	2.9E−09	7.3E−09	5.8E−08	1.4E−07	0.0E+00
225–230	0.0E+00	0.0E+00	0.0E+00	0.0E+00	0.0E+00	1.3E−10	2.4E−09	6.6E−09	5.0E−08	1.2E−07	0.0E+00

Table 3. Magnitude-distance scenarios with similar contributions to $Sa(T = 1\,\mathrm{s})$ hazard but different occurrence rates and conditional probability of causing exceedance of $sa_{T_r=475}$ in Amatrice

M	R (km)	$\nu_{R=r,M=m} \cdot \Delta m \cdot \Delta r$ (1/year)	$P[Sa(T = 1\,\mathrm{s}) > sa_{T_r=475} \mid M = m, R = r]$	$\lambda_{Sa(T=1s)>sa_{T_r=475},M=m,R=r} \cdot \Delta m \cdot \Delta r$ (1/year)
5.65–5.95	5–10	2.9E–4	1.0E–1	2.9E–5
6.85–7.15	5–10	3.8E–5	8.7E–1	3.4E–5

It immediately follows from this reasoning that, when either a distant earthquake or one of the more frequent close-by earthquakes occur, the UHS is unlikely to be exceeded. On the other hand, when a rarer earthquake occurs close to the site, it can be very likely to almost certain, depending on the magnitude, that it will cause exceedance. Therefore, the UHS may not represent a high threshold, that is, it is expected to have a high probability of being exceeded, given the occurrence of this kind of earthquakes.

Because $M = 7$ is relatively close to the maximum magnitude considered in the PSHA for Amatrice (see Table 1), one could argue that a large conditional exceedance probability is somewhat expected for such an event occurring near the site. At this point, it is crucial for the purposes of this opinion paper to also note that earthquakes of considerably lower magnitude can have high probability of exceeding the design actions if they occur near the site. A relevant example in this sense is the earthquake scenario $\Delta m \equiv 5.95 \leq M < 6.25$ (i.e., $M \approx 6.1$) and $\Delta r \equiv 0\,\mathrm{km} \leq R < 5\,\mathrm{km}$ (i.e., $R \approx 2\,\mathrm{km}$). From Table 2, this bin has a rate of exceeding the UHS $\lambda_{Sa(T=1\,\mathrm{s})>sa_{T_r=475},M=m,R=r} \cdot \Delta m \cdot \Delta r \approx 1\mathrm{E}-5$; in other words, it causes exceedance once in 100,000 years on average. On the other hand, it can be seen from Figure 3b that, in case of occurrence, it has a probability of exceeding the UHS at the $Sa(T = 1\,\mathrm{s})$ ordinate larger than 50%. This means that such a small rate of exceedance is basically warranted by the rarity of $M \approx 6.1$ at $R \approx 2\,\mathrm{km}$ from the site. Even the event that contributes most to the hazard, that is, $\Delta m \equiv 6.55 \leq M < 6.85$ at $\Delta r \equiv 10\,\mathrm{km} \leq R < 15\,\mathrm{km}$, for which $\lambda_{Sa(T=1\,\mathrm{s})>sa_{T_r=475},M=m,R=r} \cdot \Delta m \cdot \Delta r \approx 1\mathrm{E}-4$ (see Table 2), has a probability of exceeding the threshold, upon occurrence, equal to 55%; i.e., exceedance is more likely than nonexceedance.

This whole reasoning does not call into question the fact that the ordinates of the UHS for the site are exceeded, as intended, once every 475 years on average; in fact, the discussion assumes that the UHS has been accurately evaluated. It is only highlighted that this return period is warranted by the fact that the occurrence close to the site of some magnitudes, even those that are not very large, is unlikely. When such events occur near the site, exceedance of design actions can be probable to very probable. Therefore, exceedances of UHS in the epicentral areas of events, even of a magnitude relatively far from the maximum magnitude considered in hazard assessment, cannot justify surprise in the engineering community, because the spectrum is likely an easy-to-surpass threshold for these events.

Finally, note that similar reasoning can be applied to any other spectral ordinate or return period, although the range of scenarios to which it applies is expected to change in the same

way disaggregation changes with the spectral ordinate and the return period under consideration (see Iervolino et al. 2011 for a discussion with respect to Italy).

WHAT TO EXPECT IN THE EPICENTRAL AREA OF A MW 6.5 EARTHQUAKE

In light of all that was shown above, one may now return to examine what happened at Amatrice. In fact, the actual earthquake, having occurred at about 10 km from AMT, was somewhat likely to provoke exceedance of the $T_r = 475$ years UHS. The GMPE of Ambraseys et al. (1996) reveals that, for an earthquake of magnitude 6.5 at 10 km, the probability $P[Sa(T) > sa_{T_r=475} \mid M = m, R = r]$ is about 70% for the peak ground acceleration (PGA) and about 60% for the $Sa(T = 1\,\mathrm{s})$ of Figure 2b. Therefore, exceedance of the $T_r = 475$ years PGA, observed in Figure 1a, is in accord with the models underlying hazard analysis; in fact, exceedance of $Sa(T = 1\,\mathrm{s})$ could also have been expected.

The discussion given for AMT can be extended for the entire epicentral area of the earthquake. To identify the locations where exceedance of design actions should have been expected, one should examine Figure 4. The first thing shown in the figure is the surface projection of the rupture that caused the earthquake (dash-dot line) and the administrative limits of the area's municipalities (gray lines). In the same figure, the $T_r = 475$ years official elastic design actions, that is, $sa_{T_r=475}$ from Stucchi et al. (2011), are shown as colored contours for two spectral ordinates: $Sa(T = 0\,\mathrm{s})$, that is, PGA in Figure 4a and $Sa(T = 1\,\mathrm{s})$ in

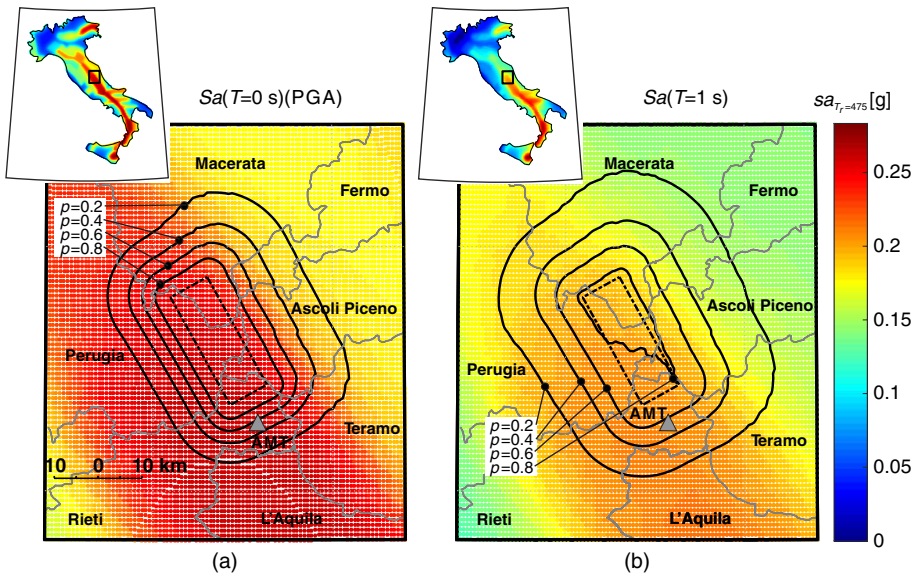

Figure 4. Design actions in terms of (a) PGA and (b) $Sa(T = 1\,s)$ for the area hit by the 30 October 2016 Mw 6.5 earthquake and exceedance probability contours conditional to the occurrence of an earthquake with the same magnitude and location. The inset maps in panels (a) and (b) are the nationwide $sa_{T_r=475}$ maps from which the main panels are extracted; figure adapted from Iervolino et al. (2017).

Figure 4b. The NTC design acceleration map refers to A-type site conditions (according to EC8 classification) for all sites. The black lines delimit areas that exhibit various probabilities $p = P[Sa(T) > sa_{T_r=475} \,|\, M = 6.5, R = r]$ of observing the exceedance of NTC design actions that are represented by the underlying colored contours (the results from the examples shown earlier in this study are not identical to the official NTC design accelerations in Figure 4 because of the simplified, single-branch, logic tree used herein). The probabilities were calculated using the GMPE of Ambraseys et al. (1996), one of the GMPEs employed when determining the code design actions of the underlying map, so that the calculations are consistent.

One notes that, although the conditional probability of exceedance rapidly decreases when moving away from the rupture, in a relatively wide area around the source, the exceedance of design actions was more likely than nonexceedance (e.g., larger than 50%) for an earthquake of the magnitude and location that occurred on 30 October 2016. As argued for the individual case of the AMT site, this by no means contradicts the hazard map but is rather an intrinsic characteristic thereof.

EARTHQUAKES LIKELY EXCEEDING DESIGN ACTIONS IN ITALY

To complete the discussion, this section reports the calculation, for any site in Italy, of the minimum magnitude that has a probability larger than 50% of causing exceedance of $sa_{T_r=475}$, in case of occurrence within 5 km from the site. These magnitudes are interesting in the sense that they represent the close-by scenarios for which it would be rational to expect exceedance of design actions rather than nonexceedance for the spectral ordinate of interest. To calculate the map, the Italian territory and the seismic source zones are discretized by a grid of 0.02° spacing. For each point $sa_{T_r=475}$, in terms of $Sa(T = 0\,\mathrm{s})$ and $Sa(T = 1\,\mathrm{s})$, is computed according to Equation 1 and using the models of the branch 921 already described. Then for each source zone, the magnitude variable, in the $(m_{\min}, m_{\max})$ interval from Table 1, is discretized with 0.1 step. For each magnitude value, the probability of exceedance is computed via Equation 5, where $f_{R\,|\,R\le 5\,\mathrm{km}}(r)$ is the source-to-site distance distribution conditional to earthquake occurrence within 5 km of the site in question (accounting for all the seismic source zones that are within 5 km).

$$P[Sa(T) > sa_{T_r=475} \,|\, M = m, R \le 5\,\mathrm{km}] = \int_0^{5\,\mathrm{km}} P[Sa(T) > sa_{T_r=475} \,|\, M = m, R = r] \cdot f_{R\,|\,R\le 5\,\mathrm{km}}(r) \cdot dr \quad (5)$$

Figure 5 reports, for each site, the minimum magnitude for which $P[Sa(T) > sa_{T_r=475} \,|\, M = m, R \le 5\,\mathrm{km}] > 0.5$. It appears that, in many cases, the lowest-magnitude events for which exceedance of design actions is more probable than not are relatively far from the maximum magnitude of the zone in which the site is enclosed (see Table 1). This is also true for $Sa(T = 1\,\mathrm{s})$, even if, as expected, such magnitudes are in general larger than those for PGA.

The maps show that the largest magnitude across Italy is $M \approx 6$, which corresponds to the most hazardous region. Therefore, an earthquake of this magnitude, wherever it occurs, has

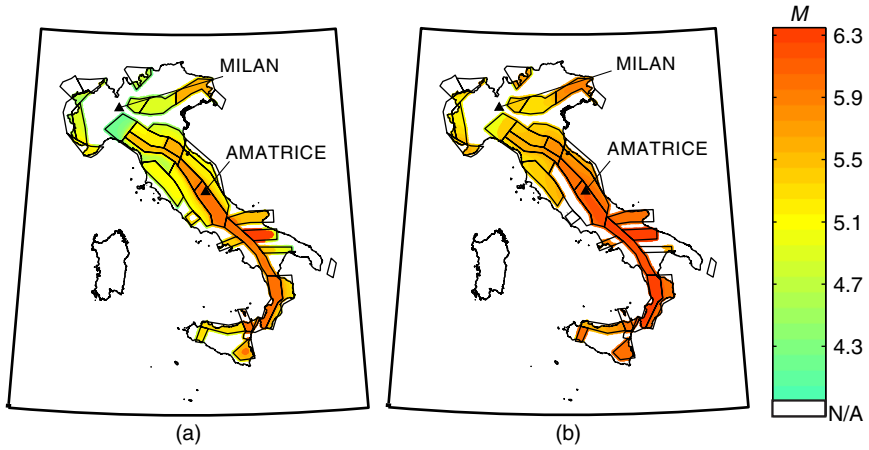

Figure 5. Minimum magnitude with probability larger than 0.5 of exceeding $sa_{T_r=475}$ if occurring within 5 km from the site. (a) PGA; (b) is $Sa(T = 1\,\mathrm{s})$. White areas correspond to sites where no earthquakes can occur within 5 km according to Meletti et al. (2008) or for which no magnitudes reach 50% probability of exceedance.

probability > 0.5 of causing exceedance in its epicentral area. Then, because earthquakes of magnitude larger than 6 have rates of 0.12 in the country (based on the same data of Table 1 extended to the full source model of Italy), meaning a return period of 8.6 years, exceedances are expected all over in Italy with a return period comparable to this one.

To get a sense of these results, it is worthwhile to focus again on Amatrice. In the case of this site, which is exposed to high hazard in Italy and is contained in zone 923, which has maximum magnitude well above $M = 7$ (see Table 1), the minimum M for which $P[Sa(T) > sa_{T_r=475} \,|\, M = m, R \leq 5\,\mathrm{km}] > 0.5$ are 6.0 and 6.1 for PGA and $Sa(T = 1\,\mathrm{s})$, respectively. It is relevant to identify these events, because exceedance of design actions is expected in case of their occurrence close to the site.

Finally, the fact that the minimum M to likely cause exceedance in AMT is larger for $Sa(T = 1\,\mathrm{s})$ than for PGA also helps to explain why the recorded spectral ordinates at the longer periods given in Figure 1a are below the code spectrum. In fact, one should still expect to very likely exceed these ordinates in some close-by earthquakes, even if correctly contemplated by PSHA, yet they should be of larger magnitude than that of the earthquake the figure refers to (as hazard disaggregation generally suggests).

It is also interesting to discuss the case of Milan (Figure 6), which is outside the zones of the model considered for the hazard assessment. This site corresponds to the white color in Figure 5, which means that there is no close-by scenario that has a conditional probability larger than 50% of causing exceedance of the PGA and $Sa(T = 1\,\mathrm{s})$ ordinates of its $T_r = 475$ years UHS. This can be better appreciated in Figure 6, which, analogous to Figure 3 for Amatrice, provides a dissection of the hazard integral for the $Sa(T = 1\,\mathrm{s})$ ordinate, which yields $sa_{T_r=475} = 0.036\,\mathrm{g}$ on A-type site class. Once again, the sum of the contributions $\lambda_{Sa(T=1\,\mathrm{s})>sa_{T_r=475},M=m,R=r} \cdot \Delta m \cdot \Delta r$ in Figure 6c provides 0.0021; however, there are no

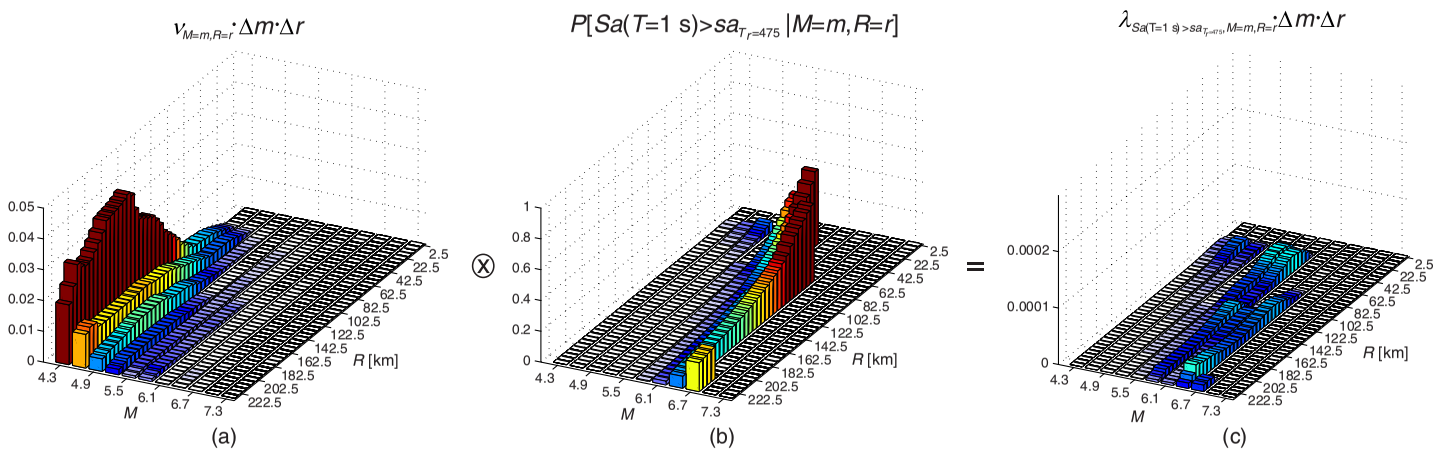

Figure 6. Magnitude and distance dissection of the hazard for Milan in terms of $T = 1$ s spectral acceleration with exceedance return period equal to 475 years, that is, 0.036 g. (a) Rates of occurrence (1/year); (b) probability of exceedance (conditional probabilities for scenarios that have 0 occurrence rate in (a) are set equal to 0 for readability); (c) product of the previous two (1/year). Integrating (c) yields 0.0021=1/475. Distance in the graphs is epicentral.

contributions from earthquakes closer than 20 km, because, as mentioned, Milan is outside the source zones considered in PSHA; see $\nu_{M=m,R=r} \cdot \Delta m \cdot \Delta r$ in Figure 6a.

Consequently, Figure 6c shows that there is no scenario dominating the hazard (i.e., the contributions are comparable for many scenarios, such that the earthquake dominating the hazard disaggregation is less straightforward to identify). Moreover, none of them has exceedance probability, conditional to occurrence (Figure 6b), larger than 50%. In fact, 49% corresponds to an $M \approx 5.8$ earthquake occurring at $R \approx 27$ km, while 50% is the maximum and corresponds to $M \approx 6.4$ at $R \approx 70$ km. In Milan, the $T_r = 475$ years UHS is harder to surpass for all the scenarios contemplated by PSHA; its exceedance can be solely due to a relatively anomalous ground motion from one of the possible scenarios, while in Amatrice, exceedance is likely due to a less anomalous shaking from a scenario whose occurrence near the site is rare. This is equivalent to saying that epsilon from disaggregation of the 475-year hazard shows larger values for Milan than Amatrice, as it happens in fact; see Iervolino et al. (2011).

FINAL REMARKS

Not questioning PSHA, which is the rational way to quantify the seismic threat for the site, this article recalled some basic arguments regarding which earthquake scenarios are likely to cause exceedance of design (probabilistic hazard–based) spectra. The discussion is related to which earthquakes can likely cause exceedance of design actions and what to expect for new structures found in the epicentral areas of these earthquakes with respect to the elastic seismic actions with which they were designed. The considerations below are worth recalling.

1. The earthquakes that occur more frequently near the site of interest and all the distant earthquakes, even of high magnitude, are unlikely to exceed the UHS; on the other hand, the events rarest to occur close can have a probability of exceedance, conditional to occurrence, that approaches 1 (i.e., exceedance can be relatively certain).
2. Rarity does not necessarily mean very large magnitude; in fact, the earthquakes for which exceedance is more likely than not, that is, those with conditional exceedance probability larger than 50% if occurring close, can be far from the maximum magnitude considered in the hazard assessment for the site.
3. For these events, which in large regions can be observed relatively frequently with respect to the return period of the UHS, exceedance is expected in an area around the source that can be, depending on the magnitude, relatively wide.

In conclusion, UHS work exactly as intended: they are such that the construction site will rarely experience accelerations exceeding them (e.g., on average, once every 475 years). At the same time, exceedances cannot be deemed rare and do not justify surprise, because earthquakes that have probability of causing exceedance of design spectra larger than 50% occur over large regions far more frequently than once in 475 years (e.g., every 10 years on average), and they will always have an epicentral area where design spectra likely represent a threshold that is relatively easy to surpass. Although exceedance does not necessarily imply violation of the design limit state, it should be made clear that, in these cases, the seismic structural safety inherent to design will be likely left to further safety margins beyond the elastic design actions, which, to date, are generally not explicitly controlled in codes.

ACKNOWLEDGMENTS

This article was developed within the activities of the ReLUIS-DPC 2014–2018 research project, funded by Presidenza del Consiglio dei Ministri, Dipartimento della Protezione Civile. The opinion and conclusions of this work do not necessarily reflect those of the funding entity. The authors thank Racquel K. Hagen (Stanford University) for having proofread the paper.

REFERENCES

Ambraseys, N. N., Simpson, K. A., and Bommer, J. J., 1996. Prediction of horizontal response spectra in Europe, *Earthquake Engineering and Structural Dynamics* **25**, 371–400.

Bommer, J. J., and Acevedo, A. B., 2004. The use of real earthquake accelerograms as input to dynamic analysis, *Journal of Earthquake Engineering* **8**, 43–91.

Chioccarelli, E., Cito, P., Iervolino, I., and Giorgio, M., 2019. REASSESS V2.0: Software for single- and multi-site probabilistic seismic hazard analysis, *Bulletin of Earthquake Engineering* **17**, 1769–1793.

Chioccarelli, E., De Luca, F., and Iervolino, I., 2012. Preliminary study of Emilia (May 20th 2012) earthquake ground motion records V2.11, available at www.reluis.it (last accessed March 2018).

Chioccarelli, E., and Iervolino, I., 2013. Near-source seismic hazard and design scenarios, *Earthquake Engineering and Structural Dynamics* **42**, 603–622.

Cornell, C. A., 1968. Engineering seismic risk analysis, *Bulletin of the Seismological Society of America* **58**, 1583–1606.

CS.LL.PP., 2008. DM 14 gennaio 2008, Norme tecniche per le costruzioni, *Gazzetta Ufficiale della Repubblica Italiana* **29**.

Dolce, M., 2011. Qui DPC: il monitoraggio sismico del dipartimento della protezione civile, *Progettazione Sismica* **3**, 95–98 (in Italian).

European Committee for Standardization (CEN), 2004. *Eurocode 8: Design Provisions for Earthquake Resistance of Structures, Part 1.1: General Rules, Seismic Actions and Rules for Buildings, BS EN 1998-1:2004*, Bruxelles, Belgium.

Gutenberg, B., and Richter, C. F., 1944. Frequency of earthquakes in California, *Bulletin of the Seismological Society of America* **34**, 185–188.

Iervolino, I., 2013. Probabilities and fallacies: Why hazard maps cannot be validated by individual earthquakes, *Earthquake Spectra* **29**, 1125–1136.

Iervolino, I., Baltzopoulos, G., Chioccarelli, E., and Suzuki, A., 2017. Seismic actions on structures in the near-source region of the 2016 central Italy sequence, *Bulletin of Earthquake Engineering*, https://doi.org/10.1007/s10518-017-0295-3 (in press).

Iervolino, I., Chioccarelli, E., and Convertito, V., 2011. Engineering design earthquakes from multimodal hazard disaggregation, *Soil Dynamics and Earthquake Engineering* **31**, 1212–1231.

Iervolino, I., and Giorgio, M., 2017. É possibile evitare il superamento delle azioni di progetto nell'area epicentrale di terremoti forti?, *Progettazione Sismica* **8**, 25–32 (in Italian).

Iervolino, I., Spillatura, A., and Bazzurro, P., 2017. RINTC project: Assessing the (implicit) seismic risk of code-conforming structures in Italy, in *Proceedings, COMPDYN 2017, 6th*

ECCOMAS Thematic Conference on Computational Methods in Structural Dynamics and Earthquake Engineering, M. Papadrakakis and M. Fragiadakis (eds.), Island of Rhodes, Greece.

Joyner, W. B., and Boore, D. M., 1981. Peak horizontal acceleration and velocity from strong motion records including records from the 1979 Imperial Valley, California, Earthquake, *Bulletin of the Seismological Society of America* **71**, 2011–2038.

Luzi., L., Hailemikael., S., Bindi, D., Pacor, F., Mele, F., and Sabetta, F., 2008. ITACA (ITalian ACcelerometric Archive): A web portal for the dissemination of Italian strong-motion data, *Seismological Research Letters* **79**, 716–722.

Luzi., L., Pacor, F., Puglia, R., Lanzano, G., Felicetta, C., D'Amico, M., Michelini, A., Faenza, L., Lauciani, V., Iervolino, I., Baltzopoulos, G., and Chioccarelli, E., 2017. The Central Italy seismic sequence between August and December 2016: Analysis of strong-motion observations, *Seismological Research Letters* **88**, 1219–1231.

Masi, A., Chiauzzi, L., Braga, F., Mucciarelli, M., Vona, M., and Ditommaso, R., 2011. Peak and integral seismic parameters of L'Aquila 2009 ground motions: Observed versus code provision values, *Bulletin of Earthquake Engineering* **9**, 139–156.

McGuire, R. K., 2004. *Seismic Hazard and Risk Analysis*, Earthquake Engineering Research Institute, Oakland, CA, 240 pp.

Meletti, C., Galadini, F., Valensise, G., Stucchi, M., Basili, R., Barba, S., Vannucci, G., and Boschi, E., 2008. A seismic source zone model for the seismic hazard assessment of the Italian territory, *Tectonophysics* **450**, 85–108.

Panza, G., Kossobokov, V. G., Peresan, A., and Nekrasova, A., 2014. Why are the standard probabilistic methods of estimating seismic hazard and risks too often wrong, in *Earthquake Hazard, Risk and Disasters* (J. F. Shroder and Max Wyss, eds.), Elsevier, Waltham, MA, 309–357.

Rovida, A. N., Locati, M., Camassi, R. D., Lolli, B., and Gasperini, P., 2016. Catalogo Parametrico dei Terremoti Italiani, versione CPTI15, available at http://emidius.mi.ingv.it/CPTI15-DBMI15/ (last accessed March 2018) (in Italian).

Stucchi, M., Meletti, C., Montaldo, V., Crowley, H., Calvi, G. M., and Boschi, E., 2011. Seismic hazard assessment (2003–2009) for the Italian Building Code, *Bulletin of the Seismological Society of America* **101**, 1885–1911.

Zanini, M. A., and Hofer, L., 2017. Sulla percezione dell'affidabilità delle stime di pericolosità sismica utilizzate nella progettazione delle strutture, *Gruppo Nazionale di Geofisica della Terra Solida GNGTS, 36° Convegno Nazionale*, Trieste, Italy, 308–311.

(Received 23 March 2018; Accepted 28 January 2019)